

Analysis of three-body charmed B meson decays $B \rightarrow D(V^* \rightarrow)VP$

Jing Ou-Yang, Run-Hui Li, Si-Hong Zhou*

Inner Mongolia Key Laboratory of Microscale Physics and Atom Innovation,

School of Physical Science and Technology,

Inner Mongolia University, Hohhot 010021, China and

Center for Quantum Physics and Technologies,

School of Physical Science and Technology,

Inner Mongolia University, Hohhot 010021, China

(Dated: June 18, 2025)

Abstract

We systematically analyze the decays $B_{(s)} \rightarrow D_{(s)}(V^* \rightarrow)VP$, where V^* represents a vector resonance (ρ , ω or K^*), and VP denotes the final-state meson pairs $\omega\pi$, $\rho\pi$ and ρK . The intermediate subprocesses $B_{(s)} \rightarrow D_{(s)}V^*$ are calculated in the factorization-assisted topological-amplitude approach, while the intermediate resonant states V^* are modeled using a relativistic Breit-Wigner distribution, subsequently decaying into VP through strong interactions. We predict the off-shell effects of the ground-state resonances (ρ , ω , K^*) in $B_{(s)} \rightarrow D_{(s)}(V^* \rightarrow)VP$. Our results show that the virtual contributions from $\rho \rightarrow \omega\pi$, $\omega \rightarrow \rho\pi$, and $K^* \rightarrow \rho K$ are crucial for these three-body decays, $B_{(s)} \rightarrow D_{(s)}VP$. In particular, the branching fractions arising from the ρ and ω virtual effects can be comparable to the total decay rates of $B_{(s)} \rightarrow D_{(s)}\omega\pi$ and $B_{(s)} \rightarrow D_{(s)}\rho\pi$, respectively. Decays with branching fractions of order $10^{-6} - 10^{-4}$ are expected to be measurable at Belle II and LHCb. Compared with previous perturbative QCD predictions for $B_{(s)} \rightarrow D_{(s)}(\rho \rightarrow)\omega\pi$, our results are consistent but exhibit higher precision.

* corresponding author: shzhou@imu.edu.cn

I. INTRODUCTION

Three-body nonleptonic B meson decays broaden the study of B decay mechanisms, enabling tests of the standard model (SM) and investigations into the emergence of quantum chromodynamics. These decays also provide additional possibilities for CP violation searches through interference between different resonant states, complementing tree and penguin amplitude interference observed in two-body B decays. The complex kinematics and phase space distributions in three-body decays are typically analyzed using Dalitz plot technique [1]. In the edges of the Dalitz plot, the invariant mass squared of two final-state particles often peaks, revealing intermediate resonances. These resonance structures provide valuable opportunities to explore the spectroscopic properties of resonant systems.

Experimentally, the branching fractions and CP asymmetries of three-body B meson decays have been precisely measured by BABAR, Belle (II) and LHCb collaborations [2–9]. Through amplitude analysis in isobar model, the fit fractions of both resonant and nonresonant components can be determined. In this framework, resonances are typically parameterized using the relativistic Breit-Wigner (RBW) lineshape, while nonresonant contributions are described by exponential distributions. This analysis provides crucial information on their corresponding ground and excited resonant states, including their masses, spin-parity quantum numbers, and other spectroscopic properties.

However, theoretical frameworks remain challenged by nonfactorizable multibody correlations, such as final-state rescattering effects [10, 11], three-body effects in final states [12, 13], and also the complex interplay between continuum and resonant states in three-body phase space. In the preliminary study of three-body effects, the heavy meson chiral perturbation theory [14–16] have been applied to calculate the nonresonant contributions in three-body charmless B meson decays, such as $B \rightarrow KKK$, $B \rightarrow K\pi\pi$ processes that are dominated by nonresonant components [17]. Actually, theoretical interest primarily focus on the resonant components of three-body B decays, where two final particles from an intermediate resonance that recoils against the third “bachelor” meson. This configuration, known as quasi-two-body decay, benefits from the large energy release in B meson decays, where the energetic resonant meson pair and bachelor meson move fast back-to-back in the B meson rest frame. This kinematic configuration naturally suppresses interactions between the meson pair and bachelor particle through power suppression, analogous to the “color trans-

parency” phenomenon observed in two-body B meson decays. This suppression enables factorization-based approaches for quasi-two-body decays, including the QCD Factorization (QCDF) [14–16, 18, 19], the PQCD approach [20–36] and factorization-assisted topological-amplitude (FAT) approach [37–41].

In this work, we concentrate on three-body charmed B decays $B_{(s)} \rightarrow D_{(s)}(V^* \rightarrow)VP$, where V^* represents the ground-state resonances ρ , ω and K^* , and VP meson pair, originating from ρ , ω and K^* intermediate resonances, denotes the $\omega\pi$, $\rho\pi$ and ρK pairs, respectively. Since the pole mass of $\rho(770)$ ($\omega(782)$, $K(892)^*$) lies below the invariant mass threshold of the $\omega\pi$ ($\rho\pi$, ρK) pair, the decays $\rho \rightarrow \omega\pi^-$ ($\omega \rightarrow \rho\pi$, $K^* \rightarrow \rho K$) can only proceed via the off-shell effects [42] through the Breit-Wigner tail (BWT) distribution. Nevertheless, this virtual effect in the $B^0 \rightarrow \bar{D}^{(*)-}\omega\pi^-$ decay was observed to be significant by Belle, with a branching fraction measured as $\mathcal{B}(B^0 \rightarrow \bar{D}^{*-}(\rho(770)^+ \rightarrow)\omega\pi^-) = (1.48_{-0.63}^{+0.37}) \times 10^{-3}$, which is comparable to $\mathcal{B}(B^0 \rightarrow \bar{D}^{*-}(\rho(1450)^+ \rightarrow)\omega\pi^-) = (1.07_{-0.34}^{+0.40}) \times 10^{-3}$ [43]. The off-shell effect of $\rho(770)^+ \rightarrow \omega\pi^-$ also plays an important role in other processes, such as $e^+e^- \rightarrow \omega\pi^0$ [44–46] and $\tau \rightarrow \omega\pi\nu_\tau$ [47]. Although there are no data for any branching fractions of $B \rightarrow D(\omega \rightarrow)\rho\pi$ and $B \rightarrow D(K^* \rightarrow)\rho K$ decays available, the existing experimental analysis for $\omega \rightarrow \pi^+\pi^-\pi^0$ decay supports the Gell-Mann-Sharp-Wagner (GSW) mechanism [48] that the $\omega \rightarrow 3\pi$ decay proceeds predominantly through intermediate $\omega \rightarrow \rho\pi$ transition, followed by the $\rho \rightarrow \pi\pi$ decay. The GSW mechanism explains the dominance of $\omega \rightarrow 3\pi$ via $\rho\pi$ intermediate state, and this likely extends to $B \rightarrow D(\omega \rightarrow)\rho\pi$ decays, though no direct measurements exist. For the $K^* \rightarrow K(\rho \rightarrow)\pi\pi$ decays only upper limits exist in experimental, theoretical estimates would require modeling of the suppressed transitions in $B \rightarrow D(K^* \rightarrow)\rho K$ firstly. The theoretical analysis of the process $B^0 \rightarrow D^{*-}\omega\pi$ has been done in Refs. [49, 50] using the factorization hypothesis, but without providing observable predictions for its branching fraction. Recently, the branching fractions of $B_{(s)} \rightarrow D_{(s)}^{(*)}(\rho(770, 1450)^+ \rightarrow)\omega\pi^+$ have been calculated within the PQCD approach [51]. Actually, the off-shell effects in $B \rightarrow DPP$ through $D^* \rightarrow DP$ have already been found to be essential for the total amplitudes by Belle [52], BABAR [3] and LHCb [6, 7, 42, 53, 54], and the corresponding studies on the theoretical side were performed firstly in the PQCD approach [55, 56], followed by more precise results in the FAT approach [37], which improved upon the PQCD predictions.

For a systematic study of $B_{(s)} \rightarrow D_{(s)}(V^* \rightarrow)VP$ decays, we will apply the FAT approach.

This framework was originally developed by one of us (S.-H. Z.) and collaborators [57–63] to address nonfactorizable contributions in two-body D and B meson decays, and has subsequently been successfully extended to both quasi-two-body B meson decays [37–39] and D meson decays [40]. Building upon the conventional topological diagram approach [64], the FAT approach systematically classifies decay amplitudes according to distinct electroweak Feynman diagrams but keeping the $SU(3)$ symmetry breaking effects. Specifically, we incorporate these symmetry-breaking effects into topological diagram amplitudes primarily through factorizing out form factors and decay constants, assisted by QCD factorization. The remaining nonfactorizable contributions are parameterized as a minimal set of universal parameters which are determined through a global fits to all available experimental data. This makes the FAT approach particularly powerful for providing precise decay amplitudes for intermediate two-body processes $B \rightarrow DV^*$ involving charmed final states. In our analysis of $B_{(s)} \rightarrow D_{(s)}(V^* \rightarrow)VP$ decays, we describe the subsequent strong decays of intermediate resonances to final-state meson pairs $\omega\pi$, $\rho\pi$ and ρK in terms of RBW formalism, consistent with experimental analyses.

The remainder of this paper is organized as follows. In Sec. II, we give an introduction of the theoretical framework. Numerical results and detailed discussions about $B_{(s)} \rightarrow D_{(s)}(\rho \rightarrow)\omega\pi$, $B_{(s)} \rightarrow D_{(s)}(\omega \rightarrow)\rho\pi$, and $B_{(s)} \rightarrow D_{(s)}(K^* \rightarrow)\rho K$ are collected in Sec. III. Sec. IV has our conclusions.

II. FACTORIZATION AMPLITUDES FOR TOPOLOGICAL DIAGRAMS

The charmed quasi-two-body decays $B_{(s)} \rightarrow D_{(s)}(V^* \rightarrow)PV$ proceed through two distinct stages. Initially, the $B_{(s)}$ meson decays into $D_{(s)}$ meson and an intermediate resonant state V^* . The unstable resonance V^* subsequently decays into a light pseudoscalar meson P and a vector meson V via strong interactions. At quark level, the first subprocess is induced by weak transitions $b \rightarrow cq\bar{u}$ ($q = d, s$) and $b \rightarrow uq\bar{c}$ ($q = d, s$), leading to final-state $D_{(s)}V^*$ and $\bar{D}_{(s)}V^*$, respectively. According to the weak interactions of $b \rightarrow cq\bar{u}$, the topological diagrams contributing to $\bar{B}_{(s)} \rightarrow D_{(s)}(V^* \rightarrow)PV$ can be classified into three types as listed in Fig. 1, (a) color-favored emission diagram T , (b) color-suppressed emission diagram C , and (c) W-exchange diagram E . For $\bar{B}_{(s)} \rightarrow \bar{D}_{(s)}(V^* \rightarrow)PV$, induced by $b \rightarrow uq\bar{c}$ transitions, an additional W-annihilation diagram A is included, as shown in Fig. 2.

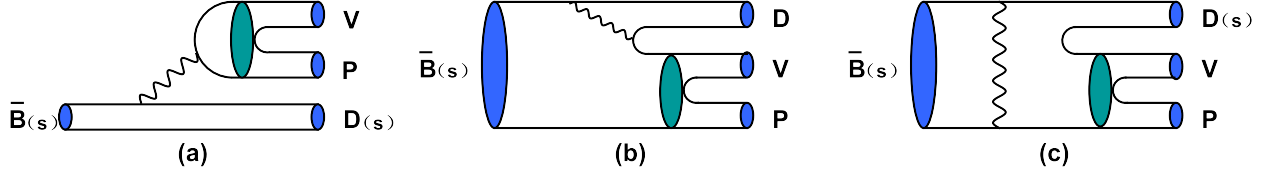


FIG. 1: Topological diagrams of $\bar{B}_{(s)} \rightarrow D_{(s)}(V^* \rightarrow)PV$ under the framework of quasi-two-body decay with the wave line representing a W boson: (a) the color-favored emission diagram T , (b) the color-suppressed emission diagram C , and (c) the W -exchange diagram E .

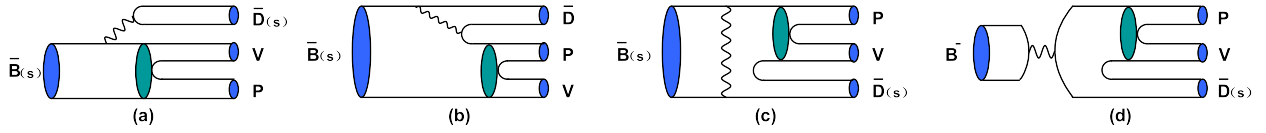


FIG. 2: The same as Fig. 1, but for $\bar{B}_{(s)} \rightarrow \bar{D}_{(s)}(V^* \rightarrow)PV$, with additional W -annihilation diagram A in (d).

The amplitudes of the first subprocess, $B_{(s)} \rightarrow D_{(s)}V^*$, can be related to those of two-body charmed B decays within the framework of the FAT approach [65]. The factorization theorem for the T diagram amplitude has been established at high precision by the QCD factorization, the perturbative QCD based on k_T factorization, as well as the soft-collinear effective theory [66–68]. Meanwhile, significant nonfactorizable effects have been observed in both the C and E topologies. Following the FAT approach [65], we parameterize the matrix elements for these nonfactorizable contributions, while adopting a well-established factorization formula for the T diagram amplitude, expressed as

$$\begin{aligned}
 T^{DV^*} &= \sqrt{2} G_F V_{cb} V_{uq}^* a_1(\mu) f_{V^*} m_{V^*} F_1^{B \rightarrow D}(m_{V^*}^2)(\varepsilon_{V^*}^* \cdot p_B), \\
 C^{DV^*} &= \sqrt{2} G_F V_{cb} V_{uq}^* f_{D(s)} m_{V^*} A_0^{B \rightarrow V^*}(m_D^2)(\varepsilon_{V^*}^* \cdot p_B) \chi^C e^{i\phi^C}, \\
 E^{DV^*} &= \sqrt{2} G_F V_{cb} V_{uq}^* m_{V^*} f_B \frac{f_{D(s)} f_{V^*}}{f_D f_\pi} (\varepsilon_{V^*}^* \cdot p_B) \chi^E e^{i\phi^E},
 \end{aligned} \tag{1}$$

where $a_1(\mu)$ in T^{DV^*} is the effective Wilson coefficient. The decay constants f_{V^*} , $f_{D(s)}$ and f_B correspond to the vector mesons, $D_{(s)}$ mesons and B mesons, respectively. The form factors $F_1^{B \rightarrow D}$ and $A_0^{B \rightarrow V^*}$ describe the $B_{(s)} \rightarrow D$ and $B_{(s)} \rightarrow V^*$ transitions amplitude, respectively. Here, $\varepsilon_{V^*}^*$ denotes the polarization vector of V^* . The parameters $\chi^{C(E)}$ and $\phi^{C(E)}$ in C^{DV^*} (E^{DV^*}) characterize the magnitude and phase of nonfactorizable contributions

after factorizing out decay constants and form factors. These unknown parameters are determined through global fits to experimental data. For Cabibbo-suppressed $\bar{B}_{(s)} \rightarrow \bar{D}_{(s)} V^*$ decays, the currently available experimental data remain insufficient to perform a global fit for extracting nonfactorizable parameters in their C and E amplitudes. We consequently use the same nonfactorizable parameters $\chi^C, \phi^C, \chi^E, \phi^E$ as in $\bar{B}_{(s)} \rightarrow D_{(s)} V^*$ decays, as done in Ref. [65]. For the A topology of $\bar{B}_{(s)} \rightarrow \bar{D}_{(s)} V^*$ decays, the dominant factorizable contribution admits a pole-model computation [65], with the explicit expression given by

$$A^{\bar{D}V^*} = -\sqrt{2} G_F V_{ub} V_{cq}^* a_1(\mu) f_B \frac{f_{D_{(s)}} g_{DDV^*} m_D^2}{m_B^2 - m_D^2} (\varepsilon_{V^*}^* \cdot p_B), \quad (2)$$

where $g_{DDV^*} = 2.52$ is the effective strong coupling constant, derived from the vector meson dominance model [69].

In the following, we will demonstrate the calculation of the subsequent subprocess, e.g., the decay of intermediate resonances into final states through strong interactions, $V^* \rightarrow PV$. The related effective Lagrangian, with strong coupling coefficient g_{V^*VP} , is written as [70–72],

$$\mathcal{L}_{V^*VP} = g_{V^*VP} \epsilon_{\mu\nu\alpha\beta} \partial^\mu V^{*\nu} \partial^\alpha V^\beta P, \quad (3)$$

and the matrix element [73–75]

$$\langle V(p_V, \lambda) P(p_P) | j_\mu(0) | 0 \rangle = i \epsilon_{\mu\nu\alpha\beta} \varepsilon^\nu(p_V, \lambda) p_P^\alpha p^\beta F_{VP}(s), \quad (4)$$

where j_μ is the isovector part of the electromagnetic current, λ is the polarization parameter. In this expression, the form factor $F_{VP}(s)$, describing $V^* \rightarrow PV$ transition, is parametrized in the vector meson dominance model as [76–79]

$$F_{VP}(s) = \frac{g_{V^*VP}}{f_{V^*}} \frac{m_{V^*}^2}{D_{V^*}(s)}. \quad (5)$$

We utilize the RBW distribution for the resonance V^* , as used in experiments [80–82]. The denominator $D_{V^*}(s)$ in Eq.(5) is given by

$$D_{V^*}(s) = m_{V^*}^2 - s - i \sqrt{s} \Gamma_{V^*}(s), \quad (6)$$

where $s = (p_P + p_V)^2$ represents the invariant mass square of the pseudoscalar and vector mesons with 4-momenta p_P, p_V . The width of vector resonances $\Gamma_{V^*}(s)$ depends on the variable s as [46],

$$\Gamma_{V^*}(s) = \Gamma_0 \frac{m_{V^*}^2}{s} \left(\frac{\mathbf{q}(s)}{\mathbf{q}_0} \right)^3 + \frac{g_{V^*VP}^2}{12\pi} \mathbf{q}^3(s), \quad (7)$$

where the first term corresponds to $V^* \rightarrow PP$ decays, and the second term describes $V^* \rightarrow VP$ decays, which are the focus of this work. Here,

$$\mathbf{q}(s) = \frac{1}{2\sqrt{s}} \sqrt{[s - (m_{pV} + m_{pP})^2][s - (m_{pV} - m_{pP})^2]}, \quad (8)$$

represents the momentum magnitude of the final state particles P or V in the rest frame of resonance V^* . The quantity \mathbf{q}_0 denotes the on-shell value of \mathbf{q} at $s = m_{V^*}^2$. In Eq. (7), Γ_0 represents the full width of the resonant state, with its value taken from the Particle Data Group (PDG) [83]. The full widths of ρ , ω , K^* , along with their corresponding resonance masses m_{V^*} , are listed in Table I.

TABLE I: Masses m_V and full widths Γ_0 (MeV) of vector resonant states.

Resonance	Line shape Parameters	Resonance	Line shape Parameters
$\rho(770)$	$m_V = 775.26 \pm 0.23$ $\Gamma_0 = 147.4 \pm 0.8$	$\omega(782)$	$m_V = 782.66 \pm 0.13$ $\Gamma_0 = 8.68 \pm 0.13$
$K^*(892)^+$	$m_V = 891.67 \pm 0.26$ $\Gamma_0 = 51.4 \pm 0.8$	$K^*(892)^0$	$m_V = 895.55 \pm 0.20$ $\Gamma_0 = 47.3 \pm 0.5$

The strong coupling constant g_{V^*VP} , defined in Eq.(3), describes the strong interactions among the three mesons at the hadron level. Its value in $V^* \rightarrow VP$ decays can be estimated using the relation $g_{V^*VP} \approx 3g_{V^*PP}^2/(8\pi^2 F_\pi)$ [84] with $F_\pi = f_\pi/\sqrt{2} = 92$ MeV [83], and $g_{\rho\pi\pi} = 6.0$, $g_{K^*K\pi} = 4.59$ [39]. Using these inputs, we obtain $g_{\rho\omega\pi} = 14.8 \text{ GeV}^{-1}$ and $g_{K^*K\rho} = 8.69 \text{ GeV}^{-1}$. The coupling $g_{\rho\omega\pi}$ has also been determined experimentally by SND Collaboration [78] yielding $15.9 \pm 0.4 \text{ GeV}^{-1}$ and $16.5 \pm 0.2 \text{ GeV}^{-1}$, depending on the form factor model used. For the numerical calculation of this work, we adopt $g_{\rho\omega\pi} = 16.0 \pm 2.0 \text{ GeV}^{-1}$, consistent with the value used in Ref. [85], to compare with the PQCD's results. The numerical results of $g_{\omega\rho\pi}$ are cited from [86] calculated by QCD sum rules, $g_{\omega\rho\pi} = 16.0 \text{ GeV}^{-1}$, which are expected to be equal to $g_{\rho\omega\pi}$ due to the similarity of the ρ and ω in the context of this vertex.

Finally, by combining the two subprocesses together, one can obtain the decay amplitudes of the topological diagrams of $B \rightarrow D(V^* \rightarrow)PV$ shown in Fig.1 and Fig.2, which are given

as follows,

$$\begin{aligned}
T &= \langle V(p_V)P(p_P)|(\bar{q}u)_{V-A}|0\rangle\langle D(p_D)|(\bar{c}b)_{V-A}|B(p_B)\rangle \\
&= \sqrt{2}G_F V_{cb}V_{uq}^* a_1 f_{V^*} m_{V^*} F_1^{B\to D}(s) \epsilon_{\mu\nu\alpha\beta} p_D^\mu \varepsilon_V^\nu p_P^\alpha (p_V + p_P)^\beta \frac{g_{V^*VP}}{D_{V^*}(s)} \\
C &= \langle V(p_V)P(p_P)|(\bar{q}b)_{V-A}|B(p_B)\rangle\langle D(p_D)|(\bar{c}u)_{V-A}|0\rangle \\
&= \sqrt{2}G_F V_{cb}V_{uq}^* f_D m_{V^*} A_0^{B\to V^*} (m_D^2) \chi^C e^{i\phi^C} \epsilon_{\mu\nu\alpha\beta} p_D^\mu \varepsilon_V^\nu p_P^\alpha (p_V + p_P)^\beta \frac{g_{V^*VP}}{D_{V^*}(s)} \\
E &= \langle D(p_D)V(p_V)P(p_P)|\mathcal{H}_{eff}|B(p_B)\rangle \\
&= \sqrt{2}G_F V_{cb}V_{uq}^* m_{V^*} f_B \frac{f_{D(s)} f_{V^*}}{f_D f_\pi} \chi^E e^{i\phi^E} \epsilon_{\mu\nu\alpha\beta} p_D^\mu \varepsilon_V^\nu p_P^\alpha (p_V + p_P)^\beta \frac{g_{V^*VP}}{D_{V^*}(s)}
\end{aligned} \tag{9}$$

for $b \rightarrow c$ transitions, and

$$\begin{aligned}
T &= \langle V(p_V)P(p_P)|(\bar{u}b)_{V-A}|B(p_B)\rangle\langle \bar{D}(p_{\bar{D}})|(\bar{c}q)_{V-A}|0\rangle \\
&= \sqrt{2}G_F V_{ub}V_{cq}^* a_1 f_D m_{V^*} A_0^{B\to V^*} (m_D^2) \epsilon_{\mu\nu\alpha\beta} p_D^\mu \varepsilon_V^\nu p_P^\alpha (p_V + p_P)^\beta \frac{g_{V^*VP}}{D_{V^*}(s)} \\
C &= \langle P(p_P)V(p_V)|(\bar{u}b)_{V-A}|B(p_B)\rangle\langle \bar{D}(p_{\bar{D}})|(\bar{c}q)_{V-A}|0\rangle \\
&= \sqrt{2}G_F V_{ub}V_{cq}^* f_D m_{V^*} A_0^{B\to V^*} (m_D^2) \chi^C e^{i\phi^C} \epsilon_{\mu\nu\alpha\beta} p_D^\mu \varepsilon_V^\nu p_P^\alpha (p_V + p_P)^\beta \frac{g_{V^*VP}}{D_{V^*}(s)} \\
E &= \langle \bar{D}(p_{\bar{D}})P(p_P)V(p_V)|\mathcal{H}_{eff}|B(p_B)\rangle \\
&= \sqrt{2}G_F V_{ub}V_{cq}^* m_{V^*} f_B \frac{f_{D(s)} f_{V^*}}{f_D f_\pi} \chi^E e^{i\phi^E} \epsilon_{\mu\nu\alpha\beta} p_D^\mu \varepsilon_V^\nu p_P^\alpha (p_V + p_P)^\beta \frac{g_{V^*VP}}{D_{V^*}(s)} \\
A &= \langle \bar{D}(p_{\bar{D}})P(p_P)V(p_V)|\mathcal{H}_{eff}|B(p_B)\rangle \\
&= \sqrt{2}G_F V_{ub}V_{cq}^* a_1 f_B \frac{f_D g_{DDV^*} m_D^2}{m_B^2 - m_D^2} \epsilon_{\mu\nu\alpha\beta} p_D^\mu \varepsilon_V^\nu p_P^\alpha (p_V + p_P)^\beta \frac{g_{V^*VP}}{D_{V^*}(s)}
\end{aligned} \tag{10}$$

for $b \rightarrow u$ transitions. Here the form factor $F_1^{B\to D}(s)$ varies dynamically with the invariant mass squared s of VP system, unlike that in two-body decays fixed at $s = m_{V^*}^2$. The decay amplitudes of $B \rightarrow DVP$ in Eq.(9) and Eq.(10) can be expressed as

$$\langle D(p_D)V(p_V)P(p_P)|\mathcal{H}_{eff}|B(p_B)\rangle = \epsilon_{\mu\nu\alpha\beta} p_D^\mu \varepsilon_V^\nu p_P^\alpha (p_V + p_P)^\beta \mathcal{A}(s), \tag{11}$$

where $\mathcal{A}(s)$ represents the sub-amplitude from Eq.(9) and Eq.(10). Using the polarization sum relation,

$$\sum_{\lambda=0,\pm} |\epsilon_{\mu\nu\alpha\beta} p_D^\mu \varepsilon_V^\nu(p_V, \lambda) p_P^\alpha (p_V + p_P)^\beta|^2 = s |\mathbf{p}_V|^2 |\mathbf{p}_D|^2 (1 - \cos^2 \theta), \tag{12}$$

we derive the differential branching fraction for $B \rightarrow DVP$, and the result is

$$\frac{d\mathcal{B}}{ds} = \frac{s |\mathbf{p}_V|^3 |\mathbf{p}_D|^3}{96\pi^3 m_B^3} \mathcal{A}(s)^2 \tau_B, \tag{13}$$

where $|\mathbf{p}_D|$ and $|\mathbf{p}_V|$ are the magnitudes of the 3-momenta p_D and p_V in the rest frame of the resonance, given by

$$|\mathbf{p}_D| = \frac{1}{2\sqrt{s}} \sqrt{(m_B^2 - m_D^2)^2 - 2(m_B^2 + m_D^2)s + s^2}, \quad (14)$$

and $|\mathbf{p}_V| = q$ [see Eq.(8)]. The quantity τ_B is the lifetime of the B meson.

III. NUMERICAL RESULTS AND DISCUSSION

A. Input parameters

The input parameters are classified into three categories:

(i) Electroweak coefficients: These contain CKM matrix elements and effective Wilson coefficients. The CKM matrix is parameterized in the Wolfenstein scheme, with parameters from PDG [83]

$$\lambda = 0.22501 \pm 0.00068, \quad A = 0.826_{-0.015}^{+0.016}, \quad \bar{\rho} = 0.1591 \pm 0.0094, \quad \bar{\eta} = 0.3523_{-0.0071}^{+0.0073}. \quad (15)$$

The effective Wilson coefficient $a_1(\mu) = C_2(\mu) + C_1/3$ is calculated as 1.036 at the scale $\mu = m_b/2$.

(ii) Hadronic parameters: The resonance mass m_{V^*} and its full width Γ_0 was listed in Table I. The strong coupling constant g_{V^*VP} involved in the resonance V^* decays was also introduced in the preceding section.

(iii) Nonperturbative QCD parameters: These include decay constants, transition form factors, and nonfactorizable parameters $\chi^{C(E)}$ and $\phi^{C(E)}$. The decay constants of pseudoscalar mesons (B, B_s, D, D_s) and light vector mesons (ρ, K^*), as well as the transition form factors $F_1(Q^2)$ and $A_0(Q^2)$ for B meson decays at zero recoil ($Q^2 = 0$), are listed in Tables II and III, respectively. The decay constants of $B_{(s)}$ and $D_{(s)}$ are derived from a

TABLE II: The decay constants of mesons (in unit of MeV).

f_B	f_{B_s}	f_D	f_{D_s}	f_ρ	f_ω	f_{K^*}
190.0 ± 1.3	230.3 ± 1.3	212.0 ± 7.0	249.9 ± 5.0	213 ± 11	192 ± 10	220 ± 11

global fit to experimental data by the PDG [83]. The decay constants of the vector mesons ρ , ω and K^* , as well as all form factors, are obtained only using various theoretical approaches,

TABLE III: The transition form factors and dipole model parameters.

	$F_1^{B \rightarrow D}$	$F_1^{B_s \rightarrow D_s}$	$A_0^{B \rightarrow \rho}$	$A_0^{B \rightarrow \omega}$	$A_0^{B \rightarrow K^*}$	$A_0^{B_s \rightarrow K^*}$
$F_i(0)$	0.54	0.58	0.30	0.26	0.33	0.27
α_1	2.44	2.44	1.56	1.60	1.51	1.74
α_2	1.49	1.70	0.17	0.22	0.14	0.47

such as light-cone sum rules [87, 88]. We utilize the same theoretical values as in our previous work on $B \rightarrow D(V \rightarrow)PP$ [39], assigning a 5% uncertainty to these decay constants and a 10% uncertainty to the form factors $F_1(0)$ and $A_0(0)$. The Q^2 -dependence of form factors can be described using various parametrizations, such as the z -series parametrization, applied to $B \rightarrow \pi, K$ [89], $B \rightarrow \rho, \omega, K^*$ [90] and $B_{(s)} \rightarrow D_{(s)}^{(*)}$ [91], and also pole model parametrization, widely used for $B_{(s)} \rightarrow V$ and $B_{(s)} \rightarrow D_{(s)}$ transitions. For (quasi-)two-body B decays, we focus on the form factors at a fixed kinematic point ($Q^2 = 0$), where the choice of parametrization has negligible impact. Following the Refs. [65] and [39], we apply the dipole model,

$$F_i(Q^2) = \frac{F_i(0)}{1 - \alpha_1 \frac{Q^2}{m_{\text{pole}}^2} + \alpha_2 \frac{Q^4}{m_{\text{pole}}^4}}, \quad (16)$$

where F_i denotes $F_{0,1}$ or A_0 , and m_{pole} is the mass of the corresponding pole state (e.g., B^* for $F_{0,1}$ and B for A_0). The dipole parameters $\alpha_{1,2}$ are given in Table III. The nonfactorizable parameters $\chi^{C(E)}$ and $\phi^{C(E)}$ in Eq.(1) were fitted with updated experimental data from PDG [83] in Ref [39], yielding

$$\begin{aligned} \chi^C &= 0.453 \pm 0.007, & \phi^C &= (65.06 \pm 0.83)^\circ, \\ \chi^E &= 0.023 \pm 0.001, & \phi^E &= (142.54 \pm 5.99)^\circ. \end{aligned} \quad (17)$$

with $\chi^2/\text{d.o.f.} = 1.6$.

By incorporating the three categories of input parameters into Eq.(13), we integrate the differential branching fraction over variable s in the whole accessible kinematic range to obtain the branching fractions for $B \rightarrow D(V^* \rightarrow)VP$ decays. Our analysis concentrate on three specific channels: $\bar{B}_{(s)} \rightarrow D_{(s)}(\rho \rightarrow)\omega\pi$, $\bar{B}_{(s)} \rightarrow D_{(s)}(\omega \rightarrow)\rho\pi$ and $\bar{B}_{(s)} \rightarrow D_{(s)}(K^* \rightarrow)\rho K$, along with their doubly CKM-suppressed counterparts $\bar{B} \rightarrow \bar{D}(V^* \rightarrow)VP$. The numerical results are collected in Tables IV – VI, respectively. The uncertainties in our predictions (\mathcal{B}_{FAT}) arise sequentially from the fitted parameters, the form factors and the decay con-

stands for $\bar{B} \rightarrow D(V^* \rightarrow)VP$, and an additional uncertainty from V_{ub} for $b \rightarrow u$ induced $\bar{B} \rightarrow \bar{D}(V^* \rightarrow)PV$ decays. The precision of these predictions can be further improved with more precise determinations of the form factors. For clarity, the three tables include the CKM matrix elements, the intermediate resonance decays, as well as the topological diagram amplitudes abbreviated as T , C , E , and A with prefactors $1, -1, \pm 1/\sqrt{2}$ for the sake of isospin and flavor mixing. The PQCD predictions are also listed in the last column of Table IV for comparison.

B. Off-shell effects of ρ , ω and K^* in $B_{(s)} \rightarrow DVP$ decays

The decay modes can be categorized based on the involved CKM matrix elements into three types: Cabibbo-favored ($V_{cb}V_{ud}^*$), Cabibbo-suppressed ($V_{cb}V_{us}^*$), and doubly Cabibbo-suppressed ($V_{ub}V_{cs}^*$ and $V_{ub}V_{cd}^*$) processes. The corresponding CKM matrix elements are listed in the second column of Tables IV – VI. This classification shows a clear hierarchy in branching fractions, where the Cabibbo-favored modes are approximately 2 – 3 orders larger than their doubly Cabibbo-suppressed counterparts within the same table. For decays governed by the same CKM matrix elements, the branching fractions also depend on the hierarchy of topological diagram amplitudes. Similar to the dynamics of the two-body B decays ($B \rightarrow DV^*$), the color-favored emission diagram (T) dominates in the quasi-two-body decays ($B \rightarrow D(V^* \rightarrow)VP$). Consequently, both the Cabibbo-favored and T diagram dominated modes are firstly to be measured experimentally. The CLEO Collaboration reported the first observation of $B^+ \rightarrow \bar{D}^0\omega\pi^+$ and $B^0 \rightarrow \bar{D}^-\omega\pi^-$ with their total branching fractions to be $(4.1 \pm 0.9) \times 10^{-3}$ and $(2.8 \pm 0.6) \times 10^{-3}$, respectively. Furthermore, a spin parity analysis of the $\omega\pi^-$ pair in the $D\omega\pi^-$ final state revealed a preference for a wide 1^- resonance [92]. In our results, the virtual ρ contributions to $\bar{B}^0 \rightarrow D^+(\rho^- \rightarrow)\omega\pi^-$ and $\bar{B}_s^0 \rightarrow D_s^+(\rho^- \rightarrow)\omega\pi^-$ modes in Tab. IV, are of nearly the same order as the total branching fractions shown above. Additionally, Ref.[43] highlights a large $\omega\pi$ contribution from $\rho(770)$ in $B^0 \rightarrow \bar{D}^{*-}\omega\pi^-$, with a measured branching fraction $\mathcal{B}(B^0 \rightarrow \bar{D}^{*-}(\rho^+ \rightarrow)\omega\pi^-) = (1.48_{-0.63}^{+0.37}) \times 10^{-3}$. Given that $B \rightarrow D(\rho \rightarrow)\omega\pi$ modes exhibit comparable virtual contribution to $B^0 \rightarrow \bar{D}^{*-}(\rho \rightarrow)\omega\pi^-$, they should also be measurable in experiments.

The processes of $B \rightarrow D(\omega \rightarrow)\rho\pi$ are listed in Table V. As the subprocesses of $\omega \rightarrow \rho^0\pi^0$, $\omega \rightarrow \rho^-\pi^+$ and $\omega \rightarrow \rho^+\pi^-$ satisfy the isospin symmetry, we only show the $B \rightarrow D(\omega \rightarrow$

) $\rho^0\pi^0$ in the table. For the decay $B \rightarrow D(\omega \rightarrow)\rho\pi$, the ω meson is produced in the initial B decays, and its subsequent decay to $\rho\pi$ would follow the Vector Meson Dominance mechanism proposed by GSW [48]. While the branching fractions for this specific decay

TABLE IV: Branching fractions in the FAT approach of quasi-two-body decays $\bar{B}_{(s)} \rightarrow D_{(s)}(\rho \rightarrow)\omega\pi$ (top) with the uncertainties from the fitted parameters, form factors and decay constants, respectively, and $\bar{B}_{(s)} \rightarrow \bar{D}_{(s)}(\rho \rightarrow)\omega\pi$ (bottom) with an additional uncertainty from V_{ub} in the last one. The PQCD predictions are also list in last column for comparison. The CKM matrix elements and topological diagram contributions denoted by T , C , E and A are listed in the second column.

Decay Modes	Amplitudes	\mathcal{B}_{FAT}	$\mathcal{B}_{\text{PQCD}}$ [85]
$\bar{B} \rightarrow D(\rho \rightarrow)\omega\pi$	$V_{cb}V_{ud}^*$	$(\times 10^{-3})$	$(\times 10^{-3})$
$B^- \rightarrow D^0(\rho^- \rightarrow)\omega\pi^-$	$T + C$	$0.80_{-0.01-0.13-0.07}^{+0.01+0.15+0.07}$	$1.42_{-0.16-0.13-0.09-0.10}^{+0.16+0.15+0.11+0.10}$
$\bar{B}^0 \rightarrow D^+(\rho^- \rightarrow)\omega\pi^-$	$T + E$	$0.54_{-0.00-0.11-0.05}^{+0.00+0.12+0.06}$	$0.80_{-0.06-0.09-0.02-0.07}^{+0.06+0.12+0.06+0.07}$
$\bar{B}^0 \rightarrow D^0(\rho^0 \rightarrow)\omega\pi^0$	$\frac{1}{\sqrt{2}}(E - C)$	$0.02_{-0.00-0.00-0.00}^{+0.00+0.00+0.00}$	
$\bar{B}_s^0 \rightarrow D_s^+(\rho^- \rightarrow)\omega\pi^-$	T	$0.68_{-0.00-0.13-0.07}^{+0.00+0.14+0.07}$	$0.88_{-0.05-0.07-0.01-0.06}^{+0.05+0.07+0.00+0.06}$
	$V_{cb}V_{us}^*$	$(\times 10^{-7})$	
$\bar{B}_s^0 \rightarrow D^+(\rho^- \rightarrow)\omega\pi^-$	E	$1.21_{-0.10-0.00-0.17}^{+0.11+0.00+0.16}$	
$\bar{B}_s^0 \rightarrow D^0(\rho^0 \rightarrow)\omega\pi^0$	$\frac{1}{\sqrt{2}}E$	$0.61_{-0.05-0-0.06}^{+0.05+0+0.07}$	
$\bar{B} \rightarrow \bar{D}(\rho \rightarrow)\omega\pi$	$V_{ub}V_{cs}^*$	$(\times 10^{-7})$	
$B^- \rightarrow D_s^-(\rho^0 \rightarrow)\omega\pi^0$	$\frac{1}{\sqrt{2}}T$	$11.05_{-0.00-2.10-0.44-0.87}^{+0.00+2.32+0.45+0.87}$	
$\bar{B}^0 \rightarrow D_s^-(\rho^+ \rightarrow)\omega\pi^+$	T	$20.21_{-0.00-3.84-0.80-1.59}^{+0.00+4.24+0.82+1.59}$	
$\bar{B}_s^0 \rightarrow D^-(\rho^+ \rightarrow)\omega\pi^+$	E	$0.12_{-0.01-0.00-0.01-0.01}^{+0.01+0.00+0.01+0.01}$	
$\bar{B}_s^0 \rightarrow \bar{D}^0(\rho^0 \rightarrow)\omega\pi^0$	$\frac{1}{\sqrt{2}}E$	$0.06_{-0.01-0.00-0.01-0.00}^{+0.01+0.00+0.01+0.00}$	
	$V_{ub}V_{cd}^*$	$(\times 10^{-7})$	
$B^- \rightarrow D^-(\rho^0 \rightarrow)\omega\pi^0$	$\frac{1}{\sqrt{2}}(T - A)$	$0.25_{-0.00-0.06-0.02-0.02}^{+0.00+0.07+0.02+0.02}$	
$B^- \rightarrow \bar{D}^0(\rho^- \rightarrow)\omega\pi^-$	$C + A$	$0.29_{-0.01-0.04-0.02-0.02}^{+0.01+0.04+0.02+0.02}$	
$\bar{B}^0 \rightarrow D^-(\rho^+ \rightarrow)\omega\pi^+$	$T + E$	$0.68_{-0.01-0.14-0.05-0.05}^{+0.01+0.15+0.05+0.05}$	
$\bar{B}^0 \rightarrow \bar{D}^0(\rho^0 \rightarrow)\omega\pi^0$	$\frac{1}{\sqrt{2}}(E - C)$	$0.14_{-0.01-0.03-0.01-0.01}^{+0.01+0.03+0.01+0.01}$	

TABLE V: Same as Table IV but for the virtual effects of $\bar{B}_{(s)} \rightarrow D_{(s)}(\omega \rightarrow)\rho\pi$.

Decay Modes	Amplitudes	\mathcal{B}_{FAT}
$\bar{B} \rightarrow D(\omega \rightarrow)\rho\pi$	$V_{cb}V_{ud}^*$	
$\bar{B}^0 \rightarrow D^0(\omega \rightarrow)\rho^0\pi^0$	$\frac{1}{\sqrt{2}}(E + C)$	$2.18_{-0.11-0.38-0.13}^{+0.11+0.19+0.14} \times 10^{-5}$
	$V_{cb}V_{us}^*$	
$\bar{B}_s^0 \rightarrow D^0(\omega \rightarrow)\rho^0\pi^0$	$\frac{1}{\sqrt{2}}E$	$5.36_{-0.46-0.00-0.56}^{+0.48+0.00+0.58} \times 10^{-8}$
$\bar{B} \rightarrow \bar{D}(\omega \rightarrow)\rho\pi$	$V_{ub}V_{cs}^*$	
$B^- \rightarrow D_s^-(\omega \rightarrow)\rho^0\pi^0$	$\frac{1}{\sqrt{2}}T$	$9.06_{-0.00-1.72-0.36-0.71}^{+0.00+1.90+0.37+0.71} \times 10^{-7}$
$\bar{B}_s^0 \rightarrow \bar{D}^0(\omega \rightarrow)\rho^0\pi^0$	$\frac{1}{\sqrt{2}}E$	$5.45_{-0.46-0.00-0.56-0.43}^{+0.48+0.00+0.59+0.43} \times 10^{-9}$
	$V_{ub}V_{cd}^*$	
$B^- \rightarrow D^-(\omega \rightarrow)\rho^0\pi^0$	$\frac{1}{\sqrt{2}}(T + A)$	$5.69_{-0.00-0.86-0.37-0.45}^{+0.00+0.93+0.38+0.45} \times 10^{-8}$
$\bar{B}^0 \rightarrow \bar{D}^0(\omega \rightarrow)\rho^0\pi^0$	$\frac{1}{\sqrt{2}}(E + C)$	$7.06_{-0.35-1.24-0.43-0.56}^{+0.35+1.37+0.44+0.56} \times 10^{-9}$

chain might not be measured, the data $\mathcal{B}(\omega \rightarrow \pi^+\pi^-\pi^0) = (89.2 \pm 0.7)\%$ [83], suggests that the subprocess $\omega \rightarrow \rho\pi$ is likely significant. Its branching fraction accounts for about 2/3 of the total decay ratio of $\omega \rightarrow 3\pi$ [93], and the contribution ratio even reach to 80% [94]. The theoretical estimates for the decay rate for $\bar{B}_{(s)} \rightarrow D_{(s)}(\omega \rightarrow)\rho\pi$ can utilize the narrow width approximation for the ω resonance, expressed as $\mathcal{B}(B \rightarrow D\omega) \times \mathcal{B}(\omega \rightarrow \rho\pi)$, where $\mathcal{B}(\omega \rightarrow \rho\pi)$ is effectively 1/2 of $\mathcal{B}(\omega \rightarrow \pi^+\pi^-\pi^0)$ without considering the interference of the respective three ρ meson [93, 94]. Taking $\bar{B}^0 \rightarrow D^0(\omega \rightarrow)\rho\pi$ as an example, its branching fraction is given by

$$\begin{aligned}
 & \mathcal{B}(\bar{B}^0 \rightarrow D^0\omega) \times \mathcal{B}(\omega \rightarrow \rho\pi) \\
 & \approx \mathcal{B}(\bar{B}^0 \rightarrow D^0\omega) \times \frac{1}{2} \mathcal{B}(\omega \rightarrow 3\pi) \\
 & = (1.16 \pm 0.25) \times 10^{-4}, \tag{18}
 \end{aligned}$$

where two-body decays is calculated to be $\mathcal{B}(\bar{B}^0 \rightarrow D^0\omega) = (2.59 \pm 0.55) \times 10^{-4}$. The value in Eq.(18) is approximately three times of the branching fraction $\mathcal{B}(\bar{B}^0 \rightarrow D^0(\omega \rightarrow)\rho^0\pi^0)$ listed in Table V, e.g., $(0.65_{-0.13}^{+0.08}) \times 10^{-4}$, by summing all $\rho\pi$ sub-channels, $\omega \rightarrow \rho^0\pi^0$, $\omega \rightarrow \rho^-\pi^+$ and $\omega \rightarrow \rho^+\pi^-$. This consistency serves as a crosscheck of the theoretical framework of FAT applied in this analysis. Experimental confirmation would require reconstructing the

TABLE VI: Same as Table IV but for the virtual effects of $\bar{B}_{(s)} \rightarrow D(K^* \rightarrow)\rho K$.

Decay Modes	Amplitudes	\mathcal{B}_{FAT}
$\bar{B} \rightarrow D(K^* \rightarrow)\rho K$	$V_{cb}V_{ud}^*$	
$\bar{B}^0 \rightarrow D_s^+(K^{*-} \rightarrow)\rho^- \bar{K}^0$	E	$0.65_{-0.06-0.00-0.08}^{+0.06+0.00+0.08} \times 10^{-6}$
$\bar{B}_s^0 \rightarrow D^0(K^{*0} \rightarrow)\rho^- K^+$	C	$1.16_{-0.04-0.22-0.08}^{+0.04+0.24+0.08} \times 10^{-5}$
	$V_{cb}V_{us}^*$	
$B^- \rightarrow D^0(K^{*-} \rightarrow)\rho^- \bar{K}^0$	$T + C$	$2.18_{-0.03-0.37-0.19}^{+0.03+0.41+0.20} \times 10^{-5}$
$\bar{B}^0 \rightarrow D^+(K^{*-} \rightarrow)\rho^- \bar{K}^0$	T	$1.64_{-0.00-0.31-0.16}^{+0.00+0.34+0.17} \times 10^{-5}$
$\bar{B}^0 \rightarrow D^0(\bar{K}^{*0} \rightarrow)\rho^+ K^-$	C	$0.79_{-0.02-0.15-0.05}^{+0.02+0.17+0.05} \times 10^{-6}$
$\bar{B}_s^0 \rightarrow D_s^+(K^{*-} \rightarrow)\rho^- \bar{K}^0$	$T + E$	$1.75_{-0.01-0.34-0.17}^{+0.01+0.38+0.18} \times 10^{-5}$
$\bar{B} \rightarrow \bar{D}(K^* \rightarrow)\rho K$	$V_{ub}V_{cs}^*$	
$B^- \rightarrow \bar{D}^0(K^{*-} \rightarrow)\rho^- \bar{K}^0$	$C + A$	$2.66_{-0.08-0.41-0.17-0.21}^{+0.08+0.45+0.18+0.21} \times 10^{-7}$
$B^- \rightarrow D^-(\bar{K}^{*0} \rightarrow)\rho^+ K^-$	A	$2.36_{-0.00-0.00-0.15-0.19}^{+0.00+0.00+0.16+0.19} \times 10^{-8}$
$\bar{B}^0 \rightarrow \bar{D}^0(\bar{K}^{*0} \rightarrow)\rho^+ K^-$	C	$1.18_{-0.04-0.22-0.08-0.09}^{+0.04+0.25+0.08+0.09} \times 10^{-7}$
$\bar{B}_s^0 \rightarrow D_s^-(K^{*+} \rightarrow)\rho^+ K^0$	$T + E$	$5.28_{-0.11-1.09-0.22-0.42}^{+0.10+1.22+0.22+0.42} \times 10^{-7}$
	$V_{ub}V_{cd}^*$	
$B^- \rightarrow D_s^-(K^{*0} \rightarrow)\rho^- K^+$	A	$1.15_{-0.00-0.00-0.08-0.09}^{+0.00+0.00+0.08+0.09} \times 10^{-9}$
$\bar{B}^0 \rightarrow D_s^-(K^{*+} \rightarrow)\rho^+ K^0$	E	$2.77_{-0.24-0.00-0.29-0.22}^{+0.25+0.00+0.31+0.22} \times 10^{-10}$
$\bar{B}_s^0 \rightarrow D^-(K^{*+} \rightarrow)\rho^+ K^0$	T	$2.52_{-0.00-0.48-0.16-0.20}^{+0.00+0.53+0.17+0.20} \times 10^{-8}$
$\bar{B}_s^0 \rightarrow \bar{D}^0(K^{*0} \rightarrow)\rho^- K^+$	C	$4.94_{-0.36-0.94-0.32-0.39}^{+0.37+1.04+0.33+0.39} \times 10^{-9}$

$\omega \rightarrow \pi^+\pi^-\pi^0$ and the $\rho \rightarrow \pi\pi$, which is challenging due to the neutral pions but feasible with high statistics datasets in Belle II and LHCb.

The $B \rightarrow D(K^* \rightarrow)\rho K$ decays are represented in Table VI. Due to isospin symmetry of strong decays, the subprocess of $B \rightarrow D(K^* \rightarrow)\rho K$ decays satisfy the following relationship,

$$\mathcal{B}(\bar{K}^{*0} \rightarrow K^- \pi^+) = 2 \mathcal{B}(\bar{K}^{*0} \rightarrow \bar{K}^0 \pi^0), \quad (19)$$

$$\mathcal{B}(K^{*-} \rightarrow \bar{K}^0 \pi^-) = 2 \mathcal{B}(K^{*-} \rightarrow K^- \pi^0), \quad (20)$$

where $\bar{K}^{*0} \rightarrow K^- \pi^+$ and $K^{*-} \rightarrow K^- \pi^0$ happen through sea quark pair $u\bar{u}$, and $\bar{K}^{*0} \rightarrow \bar{K}^0 \pi^0$ and $K^{*-} \rightarrow \bar{K}^0 \pi^-$ via $d\bar{d}$ pair. Thus, modes like $B \rightarrow D(\bar{K}^{*0} \rightarrow)\bar{K}^0 \pi^0$ and $B \rightarrow D(K^{*-} \rightarrow)$

TABLE VII: The virtual effects of $\bar{B} \rightarrow D(\rho, \omega \rightarrow) K K$ decays in the FAT approach ($\mathcal{B}_{\text{FAT}}^v$) [...].

Decay Modes	$\mathcal{B}_{\text{FAT}}^v$
$B^- \rightarrow D^0(\rho^- \rightarrow) K^- K^0$	$6.59_{-0.09}^{+0.10+1.21+0.61} \times 10^{-5}$
$\bar{B}^0 \rightarrow D^+(\rho^- \rightarrow) K^- K^0$	$4.54_{-0.03}^{+0.03+0.99+0.48} \times 10^{-5}$
$\bar{B}^0 \rightarrow D^0(\rho^0 \rightarrow) K^+ K^-$	$1.28_{-0.07}^{+0.07+0.12+0.01} \times 10^{-6}$
$\bar{B}_s^0 \rightarrow D_s^+(\rho^- \rightarrow) K^- K^0$	$5.63_{-0}^{+0+1.18+0.60} \times 10^{-5}$
$\bar{B}^0 \rightarrow D^0(\omega \rightarrow) K^+ K^-$	$1.54_{-0.07}^{+0.08+0.13+0.02} \times 10^{-6}$

$)K^- \pi^0$ need not be listed in the Table VI separately. In contrast with ω resonance, the decay $K^* \rightarrow \rho K$ is not a dominant mode. Instead, K^* typically decays via $K\pi$, e.g., $\mathcal{B}(K^{*0} \rightarrow K^+ \pi^-) \sim 100\%$. Hence no experimental data is available for $K^* \rightarrow \rho\pi$, and only the upper limits can be given for $K^{*-} \rightarrow K^- \pi^+ \pi^-$, $K^{*-} \rightarrow K^0 \pi^- \pi^0$ and $K^{*0} \rightarrow K^0 \pi^+ \pi^-$ [95]. However, as noted for the ρ resonance, they also decay to $\pi\pi$ with $\mathcal{B}(\rho \rightarrow \pi\pi) \sim 100\%$, while their off-shell effects dominate in $D\omega\pi$ final state. Following the observation of $B^+ \rightarrow \bar{D}^0 \omega \pi^+$ and $B^0 \rightarrow \bar{D}^- \omega \pi^-$ by CLEO Collaboration, we predict that the decays $B^- \rightarrow D^0(K^{*-} \rightarrow \rho^0 K^-)$ and $\bar{B}^0 \rightarrow D^+(K^{*-} \rightarrow \rho^0 K^-)$ with branching fraction of $\mathcal{O}(10^{-5})$ are also expected to be observed in future experiments. Searches for more exotic intermediate resonance decays of $K^* \rightarrow \rho K$ would require dedicated analyses by future high-statistics experiments, such as Belle II and LHCb.

In Tab. VII, we present the virtual effects of the Cabibbo-favored modes $\bar{B} \rightarrow D(\rho, \omega \rightarrow) K K$, as we calculated in Ref. [39], for comparison. A notable observation is that the off-shell effects of ρ, ω resonance in $\bar{B} \rightarrow D(\rho \rightarrow) \omega \pi$ and $\bar{B} \rightarrow D(\omega \rightarrow) \rho \pi$ are approximately two orders of magnitude larger than those in $\rho \rightarrow K K$, $\omega \rightarrow K K$, respectively. This significant difference arises primarily from the much stronger coupling strength of $\rho \rightarrow \omega \pi$ and $\omega \rightarrow \rho \pi$ ($g_{\rho\omega\pi} = 16.0 \pm 2.0 \text{ GeV}^{-1}$, $g_{\omega\rho\pi} = 16.0 \pm 2.0 \text{ GeV}^{-1}$) compared to that of $\rho \rightarrow K K$ and $\omega \rightarrow K K$ ($g_{\rho KK} = 3.2$, $g_{\omega KK} = 3.2$ [39]). These strong couplings can be calculated by some nonperturbative methods, such as QCD sum rules, so as to understand the strong decay mechanism of ρ, ω mesons.

C. Comparison with the results in the PQCD approach

Since most quasi-two-body decays $B_{(s)} \rightarrow D_{(s)}(V^* \rightarrow)PV$ have not yet been measured experimentally, we compare our results with the PQCD predictions from Ref. [85], listed in the last column of Table IV for comparison. Our calculation for $B^- \rightarrow D^0(\rho^- \rightarrow)\omega\pi^-$, $\bar{B}^0 \rightarrow D^+(\rho^- \rightarrow)\omega\pi^-$, and $\bar{B}_s^0 \rightarrow D_s^+(\rho^- \rightarrow)\omega\pi^-$ are consistent with the PQCD calculations but are in fact more precise. The PQCD results mainly includes some hadronic uncertainties, such as shape parameters ω_B and Gegenbauer moments, which are comparable to the uncertainties arising from form factors and decay constants in our analysis. However, it does not account for uncertainties from $1/m_b$ power corrections such as annihilation and hard-scattering contributions, and higher order α_s effects, which would introduce significant additional uncertainties in their results predictions, the same as in two-body decays $B \rightarrow DV^*$ [96].

Actually, in the PQCD approach, the light-cone distribution amplitude (LCDA) of the $\omega\pi$ meson pair originating from the P-wave resonance ρ can be expressed in terms of time-like form factors $F_{\omega\pi}$, parameterized using the RBW distribution. This treatment of resonant decays like $\rho \rightarrow \omega\pi$ is fully compatible with the framework of the FAT approach. The key distinction between the two methods lies in their handling of the weak decay amplitudes for $B \rightarrow DV^*$. As discussed in Sec. I, the FAT approach determines the nonperturbative parameters associated with the topological diagrams (C , E and A) by a global fit to all experimental data of $B \rightarrow DV^*$. This data-driven constraint ensures that these parameters are tightly controlled. In contrast, PQCD face large uncertainties from non-perturbative parameters as the $1/m_b$ power corrections and high order α_s effects are hard to be calculated under the PQCD framework.

Meanwhile, the hierarchy of topological amplitudes differs between the two approaches. In the FAT framework, the magnitude of C diagram amplitude is larger than that of E , i.e., $|C| > |E|$, as shown in Eq.(17). In contrast, PQCD calculations [96] yield $|C| \sim |E|$ due to the absence of power corrections and higher-order radiative contributions. It is well established that the T diagram remains factorizable to all orders in α_s for these decays, making the perturbative calculation reliable. Accordingly, our results of the T diagram dominated decay modes (listed in the top of Tables IV) align with PQCD predictions. However, for decays governed by C amplitude, especially for those with branching ratio of

$\mathcal{O}(10^{-5})$, are waiting to be tested by the future experiments and PQCD calculations.

IV. CONCLUSION

Motivated by the searches for virtual effects of intermediate resonances, we present a systematic analysis of the quasi-two-body decays $B_{(s)} \rightarrow D_{(s)}(V^* \rightarrow)VP$ where the intermediate ground states V^* are ρ , ω , K^* . These decays proceed via $b \rightarrow c$ or $b \rightarrow u$ transitions, corresponding to $\bar{B}_{(s)} \rightarrow D_{(s)}V^*$ and $\bar{B}_{(s)} \rightarrow \bar{D}_{(s)}V^*$, respectively. The resonant states V^* subsequently decay into VP pairs through strong interactions. Under the framework of FAT, we incorporate all nonperturbative contributions in $B_{(s)} \rightarrow D_{(s)}V^*$ to achieve a precise description of the first subprocess. For the intermediate resonances decays, we apply the RBW function as usually used in experiments and the PQCD approach.

We categorize $B_{(s)} \rightarrow D_{(s)}(V^* \rightarrow)VP$ into three groups according to the intermediate resonances, e.g., $B_{(s)} \rightarrow D_{(s)}(\rho \rightarrow)\omega\pi$, $B_{(s)} \rightarrow D_{(s)}(\omega \rightarrow)\rho\pi$ and $B_{(s)} \rightarrow D_{(s)}(K^* \rightarrow)\rho K$. Since the pole masses of ρ , ω , K^* lie below the invariant mass threshold of their corresponding final-state pairs, these resonances can only contribute through their BWT distribution. We calculate the branching fractions for all three decay types. Our analysis shows that the virtual contributions of ρ , ω , K^* play a crucial role in the three-body decays $B_{(s)} \rightarrow D_{(s)}VP$. Some modes exhibit decay rates up to $\mathcal{O}(10^{-4})$, comparable to their total branching fractions. For decays involving $\omega \rightarrow \rho\pi$, our results are in good agreement with the experimental analysis of $\omega \rightarrow \pi^+\pi^-\pi^0$. In particular, for $B^- \rightarrow D^0(\rho^- \rightarrow)\omega\pi^-$, $\bar{B}^0 \rightarrow D^+(\rho^- \rightarrow)\omega\pi^-$, and $\bar{B}_s^0 \rightarrow D_s^+(\rho^- \rightarrow)\omega\pi^-$ previously calculated in PQCD approach, our predictions agree with them but with smaller uncertainties. Since most quasi-two-body decays $B_{(s)} \rightarrow D_{(s)}(V^* \rightarrow)PV$ remain unmeasured experimentally. Our predictions for both the Cabibbo-favored and T diagram dominated modes with branching fractions of order $10^{-6} - 10^{-4}$ are promising targets for future high statistics experiments, such as in Belle II and LHCb.

Acknowledgments

The work is supported by the National Natural Science Foundation of China under Grants No.12465017 and No.12075126.

-
- [1] R. H. Dalitz, *Decay of tau mesons of known charge*, Phys. Rev. **94** (1954) 1046–1051.
 - [2] Belle Collaboration, A. Kuzmin et al., *Study of anti- $B^0 \rightarrow D^0\pi^+\pi^-$ decays*, Phys. Rev. D **76** (2007) 012006, [hep-ex/0611054].
 - [3] BaBar Collaboration, B. Aubert et al., *Dalitz Plot Analysis of $B \rightarrow D^+\pi^-\pi^-$* , Phys. Rev. D **79** (2009) 112004, [arXiv:0901.1291].
 - [4] BaBar Collaboration, P. del Amo Sanchez et al., *Dalitz-plot Analysis of $B^0 \rightarrow \bar{D}^0\pi^+\pi^-$* , 7, 2010. arXiv:1007.4464.
 - [5] LHCb Collaboration, R. Aaij et al., *Dalitz plot analysis of $B_s^0 \rightarrow \bar{D}^0K^-\pi^+$ decays*, Phys. Rev. D **90** (2014), no. 7 072003, [arXiv:1407.7712].
 - [6] LHCb Collaboration, R. Aaij et al., *Dalitz plot analysis of $B^0 \rightarrow \bar{D}^0\pi^+\pi^-$ decays*, Phys. Rev. D **92** (2015), no. 3 032002, [arXiv:1505.01710].
 - [7] LHCb Collaboration, R. Aaij et al., *Amplitude analysis of $B^0 \rightarrow \bar{D}^0K^+\pi^-$ decays*, Phys. Rev. D **92** (2015), no. 1 012012, [arXiv:1505.01505].
 - [8] LHCb Collaboration, R. Aaij et al., *Observation of the decay $B_s^0 \rightarrow \bar{D}^0K^+K^-$* , Phys. Rev. D **98** (2018), no. 7 072006, [arXiv:1807.01891].
 - [9] Belle-II Collaboration, F. Abudinén et al., *Observation of $B \rightarrow D^{(*)}K^-K_S^0$ decays using the 2019-2022 Belle II data sample*, [arXiv:2305.01321].
 - [10] I. Bediaga and P. C. Magalhães, *Final state interaction on $B^+ \rightarrow \pi^-\pi^+\pi^+$* , [arXiv:1512.09284].
 - [11] J. R. Pelaez and A. Rodas, *$\pi\pi \rightarrow K\bar{K}$ scattering up to 1.47 GeV with hyperbolic dispersion relations*, Eur. Phys. J. C **78** (2018), no. 11 897, [arXiv:1807.04543].
 - [12] K. S. F. F. Guimaraes, I. Bediaga, A. Delfino, T. Frederico, A. C. dos Reis, and L. Tomio, *Three-body model of the final state interaction in heavy meson decay*, Nucl. Phys. B Proc. Suppl. **199** (2010) 341–344.
 - [13] P. C. Magalhaes, M. R. Robilotta, K. S. F. F. Guimaraes, T. Frederico, W. de Paula,

- I. Bediaga, A. C. d. Reis, C. M. Maekawa, and G. R. S. Zarnauskas, *Towards three-body unitarity in $D^+ \rightarrow K^-\pi^+\pi^+$* , Phys. Rev. D **84** (2011) 094001, [arXiv:1105.5120].
- [14] H.-Y. Cheng and K.-C. Yang, *Nonresonant three-body decays of D and B mesons*, Phys. Rev. D **66** (2002) 054015, [hep-ph/0205133].
- [15] H.-Y. Cheng, C.-K. Chua, and A. Soni, *Charmless three-body decays of B mesons*, Phys. Rev. D **76** (2007) 094006, [arXiv:0704.1049].
- [16] H.-Y. Cheng and C.-K. Chua, *Branching Fractions and Direct CP Violation in Charmless Three-body Decays of B Mesons*, Phys. Rev. D **88** (2013) 114014, [arXiv:1308.5139].
- [17] H.-Y. Cheng, *Theoretical Overview of Hadronic Three-body B Decays*, [arXiv:0806.2895].
- [18] T. Huber, J. Virto, and K. K. Vos, *Three-Body Non-Leptonic Heavy-to-heavy B Decays at NNLO in QCD*, JHEP **11** (2020) 103, [arXiv:2007.08881].
- [19] X.-L. Yuan, G. Lü, N. Wang, and C. Wang, *The resonance effect for the CP asymmetry associated with the process $\omega \rightarrow \pi^+\pi^-\pi^0$* *, Chin. Phys. C **49** (2025), no. 2 023101, [arXiv:2404.01665].
- [20] C.-H. Chen and H.-n. Li, *Three body nonleptonic B decays in perturbative QCD*, Phys. Lett. B **561** (2003) 258–265, [hep-ph/0209043].
- [21] W.-F. Wang, H.-C. Hu, H.-n. Li, and C.-D. Lü, *Direct CP asymmetries of three-body B decays in perturbative QCD*, Phys. Rev. D **89** (2014), no. 7 074031, [arXiv:1402.5280].
- [22] W.-F. Wang and H.-n. Li, *Quasi-two-body decays $B \rightarrow K\rho \rightarrow K\pi\pi$ in perturbative QCD approach*, Phys. Lett. B **763** (2016) 29–39, [arXiv:1609.04614].
- [23] Y. Li, A.-J. Ma, W.-F. Wang, and Z.-J. Xiao, *Quasi-two-body decays $B_{(s)} \rightarrow P\rho \rightarrow P\pi\pi$ in perturbative QCD approach*, Phys. Rev. D **95** (2017), no. 5 056008, [arXiv:1612.05934].
- [24] Y. Li, W.-F. Wang, A.-J. Ma, and Z.-J. Xiao, *Quasi-two-body decays $B_{(s)} \rightarrow K^*(892)h \rightarrow K\pi h$ in perturbative QCD approach*, Eur. Phys. J. C **79** (2019), no. 1 37, [arXiv:1809.09816].
- [25] W.-F. Wang, *Will the subprocesses $\rho(770, 1450)^0 \rightarrow K^+K^-$ contribute large branching fractions for $B^\pm \rightarrow \pi^\pm K^+K^-$ decays?*, Phys. Rev. D **101** (2020), no. 11 111901(R), [arXiv:2004.09027].
- [26] Y.-Y. Fan and W.-F. Wang, *Resonance contributions $\phi(1020, 1680) \rightarrow K\bar{K}f$ or the three-body decays $B \rightarrow K\bar{K}h$* , Eur. Phys. J. C **80** (2020), no. 9 815, [arXiv:2006.08223].
- [27] W.-F. Wang, *Contributions for the kaon pair from $\rho(770)$, $\omega(782)$ and their excited states in*

- the $B \rightarrow K\bar{K}h$ decays, Phys. Rev. D **103** (2021), no. 5 056021, [arXiv:2012.15039].
- [28] Z.-T. Zou, Y. Li, Q.-X. Li, and X. Liu, *Resonant contributions to three-body $B \rightarrow KKK$ decays in perturbative QCD approach*, Eur. Phys. J. C **80** (2020), no. 5 394, [arXiv:2003.03754].
- [29] Z.-T. Zou, Y. Li, and X. Liu, *Branching fractions and CP asymmetries of the quasi-two-body decays in $B_s \rightarrow K^0(\bar{K}^0)K^\pm\pi^\mp$ within PQCD approach*, Eur. Phys. J. C **80** (2020), no. 6 517, [arXiv:2005.02097].
- [30] Z.-T. Zou, L. Yang, Y. Li, and X. Liu, *Study of Quasi-two-body $B_{(s)} \rightarrow \phi(f_0(980)/f_2(1270) \rightarrow)\pi\pi$ Decays in Perturbative QCD Approach*, Eur. Phys. J. C **81** (2021), no. 1 91, [arXiv:2011.07676].
- [31] L. Yang, Z.-T. Zou, Y. Li, X. Liu, and C.-H. Li, *Quasi-two-body $B_{(s)} \rightarrow V\pi\pi$ decays with resonance $f_0(980)$ in the PQCD approach*, Phys. Rev. D **103** (2021), no. 11 113005, [arXiv:2103.15031].
- [32] W.-F. Liu, Z.-T. Zou, and Y. Li, *Charmless Quasi-Two-Body B Decays in Perturbative QCD Approach: Taking $B \rightarrow K(R \rightarrow)K^+K^-$ as Examples*, Adv. High Energy Phys. **2022** (2022) 5287693, [arXiv:2112.00315].
- [33] Z.-Q. Zhang, Y.-C. Zhao, Z.-L. Guan, Z.-J. Sun, Z.-Y. Zhang, and K.-Y. He, *Quasi-two-body decays in the perturbative QCD approach**, Chin. Phys. C **46** (2022), no. 12 123105, [arXiv:2207.02043].
- [34] Z.-Y. Zhang, Z.-Q. Zhang, S.-Y. Wang, Z.-J. Sun, and Y.-Y. Yang, *Quasi-two-body decays $B_c \rightarrow K^*h \rightarrow K\pi h$ in perturbative QCD*, Phys. Rev. D **108** (2023), no. 7 076009.
- [35] Y.-C. Zhao, Z.-Q. Zhang, Z.-Y. Zhang, Z.-J. Sun, and Q.-B. Meng, *Quasi-two-body decays in perturbative QCD**, Chin. Phys. C **47** (2023), no. 7 073104, [arXiv:2304.13286].
- [36] Q. Chang, L. Yang, Z.-T. Zou, and Y. Li, *Study of the $B^+ \rightarrow \pi^+(\pi^+\pi^-)$ decay in PQCD Approach*, [arXiv:2405.15309].
- [37] S.-H. Zhou, R.-H. Li, Z.-Y. Wei, and C.-D. Lu, *Analysis of three-body charmed B-meson decays under the factorization-assisted topological-amplitude approach*, Phys. Rev. D **104** (2021), no. 11 116012, [arXiv:2107.11079].
- [38] S.-H. Zhou, X.-X. Hai, R.-H. Li, and C.-D. Lu, *Analysis of three-body charmless B-meson decays under the factorization-assisted topological-amplitude approach*, Phys. Rev. D **107** (2023), no. 11 116023, [arXiv:2305.02811].

- [39] S.-H. Zhou, R.-H. Li, and X.-Y. Lü, *Analysis of three-body decays $B \rightarrow D(V \rightarrow) PP$ under the factorization-assisted topological-amplitude approach*, Phys. Rev. D **110** (2024), no. 5 056001, [arXiv:2406.00373].
- [40] X.-D. Zhou and S.-H. Zhou, *Analysis of three-body hadronic D -meson decays*, Phys. Rev. D **111** (2025), no. 11 116008, [arXiv:2503.18593].
- [41] W.-F. Wang, J.-Y. Xu, S.-H. Zhou, and P.-P. Shi, *Contributions of $\rho(770, 1450) \rightarrow \omega\pi$ for the Cabibbo-favored $D \rightarrow h\omega\pi$ decays*, [arXiv:2502.11159].
- [42] **LHCb** Collaboration, R. Aaij et al., *Amplitude analysis of $B^- \rightarrow D^+\pi^-\pi^-$ decays*, Phys. Rev. D **94** (2016), no. 7 072001, [arXiv:1608.01289].
- [43] **Belle** Collaboration, D. Matvienko et al., *Study of D^{**} production and light hadronic states in the $\bar{B}^0 \rightarrow D^{*+}\omega\pi^-$ decay*, Phys. Rev. D **92** (2015), no. 1 012013, [arXiv:1505.03362].
- [44] **BaBar** Collaboration, J. P. Lees et al., *Measurement of the $e^+e^- \rightarrow \pi^+\pi^-\pi^0\pi^0$ cross section using initial-state radiation at BABAR*, Phys. Rev. D **96** (2017), no. 9 092009, [arXiv:1709.01171].
- [45] **BESIII** Collaboration, M. Ablikim et al., *Observation of a resonant structure in $e^+e^- \rightarrow \omega\eta$ and another in $e^+e^- \rightarrow \omega\pi^0$ at center-of-mass energies between 2.00 and 3.08 GeV*, Phys. Lett. B **813** (2021) 136059, [arXiv:2009.08099].
- [46] **SND** Collaboration, M. N. Achasov et al., *Study of the process $e^+e^- \rightarrow \omega\pi^0 \rightarrow \pi + \pi^-\pi^0\pi^0$ in the energy range 1.05–2.00 GeV with SND*, Phys. Rev. D **108** (2023), no. 9 092012, [arXiv:2309.00280].
- [47] **BaBar** Collaboration, B. Aubert et al., *Search for Second-Class Currents in $\tau^- \rightarrow \omega\pi^-\nu_\tau$* , Phys. Rev. Lett. **103** (2009) 041802, [arXiv:0904.3080].
- [48] M. Gell-Mann, D. Sharp, and W. G. Wagner, *Decay rates of neutral mesons*, Phys. Rev. Lett. **8** (1962) 261.
- [49] D. V. Matvienko, A. S. Kuzmin, and S. I. Eidelman, *A model of $\bar{B}^0 \rightarrow D^{*+}\omega\pi^-$ decay*, JHEP **09** (2011) 129, [arXiv:1108.2862].
- [50] S. I. Eidelman, L. V. Kardapoltsev, and D. V. Matvienko, *A study of the corrections to factorization in $\bar{B}^0 \rightarrow D^{*+}\omega\pi^-$* , JHEP **02** (2020) 168, [arXiv:1909.00200].
- [51] Y.-S. Ren, A.-J. Ma, and W.-F. Wang, *The $\rho(770, 1450) \rightarrow \omega\pi$ contributions for three-body decays $B \rightarrow \bar{D}^{(*)}\omega\pi$* , JHEP **01** (2024) 047, [arXiv:2311.00413].
- [52] **Belle** Collaboration, K. Abe et al., *Study of $B^- \rightarrow D^{**0}\pi^- (D^{**0} \rightarrow D^{(*)+}\pi^-)$ decays*, Phys.

- Rev. D **69** (2004) 112002, [[hep-ex/0307021](#)].
- [53] **LHCb** Collaboration, R. Aaij et al., *First observation and amplitude analysis of the $B^- \rightarrow D^+ K^- \pi^-$ decay*, Phys. Rev. D **91** (2015), no. 9 092002, [[arXiv:1503.02995](#)]. [Erratum: Phys.Rev.D 93, 119901 (2016)].
- [54] **LHCb** Collaboration, R. Aaij et al., *First observation of the rare $B^+ \rightarrow D^+ K^+ \pi^-$ decay*, Phys. Rev. D **93** (2016), no. 5 051101, [[arXiv:1512.02494](#)]. [Erratum: Phys.Rev.D 93, 119902 (2016)].
- [55] W.-F. Wang and J. Chai, *Virtual contributions from $D^*(2007)^0$ and $D^*(2010)^\pm$ in the $B \rightarrow D\pi h$ decays*, Phys. Lett. B **791** (2019) 342–350, [[arXiv:1812.08524](#)].
- [56] J. Chai, S. Cheng, and W.-F. Wang, *The role of $D_{(s)}^*$ and their contributions in $B_{(s)} \rightarrow D_{(s)} hh'$ decays*, Phys. Rev. D **103** (2021) 096016, [[arXiv:2102.04691](#)].
- [57] H.-n. Li, C.-D. Lu, and F.-S. Yu, *Branching ratios and direct CP asymmetries in $D \rightarrow PP$ decays*, Phys. Rev. D **86** (2012) 036012, [[arXiv:1203.3120](#)].
- [58] Q. Qin, H.-n. Li, C.-D. Lü, and F.-S. Yu, *Branching ratios and direct CP asymmetries in $D \rightarrow PV$ decays*, Phys. Rev. D **89** (2014), no. 5 054006, [[arXiv:1305.7021](#)].
- [59] S.-H. Zhou, Y.-B. Wei, Q. Qin, Y. Li, F.-S. Yu, and C.-D. Lu, *Analysis of Two-body Charmed B Meson Decays in Factorization-Assisted Topological-Amplitude Approach*, Phys. Rev. D **92** (2015), no. 9 094016, [[arXiv:1509.04060](#)].
- [60] S.-H. Zhou, Q.-A. Zhang, W.-R. Lyu, and C.-D. Lü, *Analysis of Charmless Two-body B decays in Factorization Assisted Topological Amplitude Approach*, Eur. Phys. J. C **77** (2017), no. 2 125, [[arXiv:1608.02819](#)].
- [61] H.-Y. Jiang, F.-S. Yu, Q. Qin, H.-n. Li, and C.-D. Lü, *$D^0-\bar{D}^0$ mixing parameter y in the factorization-assisted topological-amplitude approach*, Chin. Phys. C **42** (2018), no. 6 063101, [[arXiv:1705.07335](#)].
- [62] S.-H. Zhou and C.-D. Lü, *Extraction of the CKM phase γ from the charmless two-body B meson decays*, Chin. Phys. C **44** (2020), no. 6 063101, [[arXiv:1910.03160](#)].
- [63] Q. Qin, C. Wang, D. Wang, and S.-H. Zhou, *The factorization-assisted topological-amplitude approach and its applications*, Front. Phys. (Beijing) **18** (2023), no. 6 64602, [[arXiv:2111.14472](#)].
- [64] H.-Y. Cheng and C.-W. Chiang, *Two-body hadronic charmed meson decays*, Phys. Rev. D **81** (2010) 074021, [[arXiv:1001.0987](#)].

- [65] S.-H. Zhou, Y.-B. Wei, Q. Qin, Y. Li, F.-S. Yu, and C.-D. Lü, *Analysis of Two-body Charmed B Meson Decays in Factorization-Assisted Topological-Amplitude Approach*, Phys. Rev. D **92** (2015), no. 9 094016, [arXiv:1509.04060].
- [66] Y.-Y. Keum, T. Kurimoto, H. N. Li, C.-D. Lu, and A. I. Sanda, *Nonfactorizable contributions to $B \rightarrow D^{**(*)}M$ decays*, Phys. Rev. D **69** (2004) 094018, [hep-ph/0305335].
- [67] M. Beneke, G. Buchalla, M. Neubert, and C. T. Sachrajda, *QCD factorization for exclusive, nonleptonic B meson decays: General arguments and the case of heavy light final states*, Nucl. Phys. B **591** (2000) 313–418, [hep-ph/0006124].
- [68] C. W. Bauer, D. Pirjol, and I. W. Stewart, *A Proof of factorization for $B \rightarrow D\pi$* , Phys. Rev. Lett. **87** (2001) 201806, [hep-ph/0107002].
- [69] Z.-w. Lin and C. M. Ko, *A Model for J/ψ absorption in hadronic matter*, Phys. Rev. C **62** (2000) 034903, [nucl-th/9912046].
- [70] D. H. Boal, B. J. Edwards, A. N. Kamal, R. Rockmore, and R. Torgerson, *Vector Meson Couplings and the Observability of the $K^* \rightarrow K^+\pi^+\pi^-$ Decays*, Phys. Lett. B **66** (1977) 165–166.
- [71] O. Kaymakcalan, S. Rajeev, and J. Schechter, *Nonabelian Anomaly and Vector Meson Decays*, Phys. Rev. D **30** (1984) 594.
- [72] S. Fajfer, K. Suruliz, and R. J. Oakes, *$\tau \rightarrow \omega\pi\nu_\tau$ decay*, Phys. Rev. D **46** (1992) 1195–1197.
- [73] S. Pacetti, *A Practical guide to unravel time-like transition form-factors*, Eur. Phys. J. A **38** (2008) 331–343, [arXiv:0807.1399].
- [74] I. Caprini, *Testing the consistency of the $\omega\pi$ transition form factor with unitarity and analyticity*, Phys. Rev. D **92** (2015), no. 1 014014, [arXiv:1505.05282].
- [75] H. Schäfer, M. Zanke, Y. Korte, and B. Kubis, *The semileptonic decays $\eta^{(\prime)} \rightarrow \pi^0\ell^+\ell^-$ and $\eta' \rightarrow \eta\ell^+\ell^-$ in the standard model*, Phys. Rev. D **108** (2023), no. 7 074025, [arXiv:2307.10357].
- [76] M. N. Achasov et al., *Study of $e^+e^- \rightarrow \omega\pi^0 \rightarrow \pi^0\pi^0\gamma$ in the energy range 1.05 – 2.00 GeV with SND*, Phys. Rev. D **88** (2013), no. 5 054013, [arXiv:1303.5198].
- [77] M. N. Achasov et al., *The Process $e^+e^- \rightarrow \omega\pi^0 \rightarrow \pi^0\pi^0\gamma$ up to 1.4-GeV*, Phys. Lett. B **486** (2000) 29–34, [hep-ex/0005032].
- [78] M. N. Achasov et al., *Updated measurement of the $e^+e^- \rightarrow \omega\pi^0 \rightarrow \pi^0\pi^0\gamma$ cross section with the SND detector*, Phys. Rev. D **94** (2016), no. 11 112001, [arXiv:1610.00235].

- [79] S.-s. Fang, B. Kubis, and A. Kupsc, *What can we learn about light-meson interactions at electron-positron colliders?*, Prog. Part. Nucl. Phys. **120** (2021) 103884, [arXiv:2102.05922].
- [80] **LHCb** Collaboration, R. Aaij et al., *Amplitude analysis of the $B^+ \rightarrow \pi^+\pi^+\pi^-$ decay*, Phys. Rev. D **101** (2020), no. 1 012006, [arXiv:1909.05212].
- [81] **BaBar** Collaboration, J. P. Lees et al., *Amplitude Analysis of $B^0 \rightarrow K^+\pi^-\pi^0$ and Evidence of Direct CP Violation in $B \rightarrow K^*\pi$ decays*, Phys. Rev. D **83** (2011) 112010, [arXiv:1105.0125].
- [82] **BaBar** Collaboration, J. P. Lees et al., *Precise Measurement of the $e^+e^- \rightarrow \pi^+\pi^-(\gamma)$ Cross Section with the Initial-State Radiation Method at BABAR*, Phys. Rev. D **86** (2012) 032013, [arXiv:1205.2228].
- [83] **Particle Data Group** Collaboration, S. Navas et al., *Review of particle physics*, Phys. Rev. D **110** (2024), no. 3 030001.
- [84] D. H. Boal, B. J. Edwards, A. N. Kamal, R. Rockmore, and R. Torgerson, *Vector Meson Couplings and the Observability of the $K^* \rightarrow K\pi\pi$ Decays*, Phys. Lett. B **66** (1977) 165–166.
- [85] Y.-S. Ren, A.-J. Ma, and W.-F. Wang, *The $\rho(770, 1450) \rightarrow \omega\pi$ contributions for three-body decays $B \rightarrow \overline{D}^{(*)}\omega\pi$* , JHEP **01** (2024) 047, [arXiv:2311.00413].
- [86] M. Lublinsky, *G ($\omega\rho\pi$) reexamined*, Phys. Rev. D **55** (1997) 249–254, [hep-ph/9608331].
- [87] Y.-M. Wang and Y.-L. Shen, *QCD corrections to $B \rightarrow \pi$ form factors from light-cone sum rules*, Nucl. Phys. B **898** (2015) 563–604, [arXiv:1506.00667].
- [88] J. Gao, C.-D. Lü, Y.-L. Shen, Y.-M. Wang, and Y.-B. Wei, *Precision calculations of $B \rightarrow V$ form factors from soft-collinear effective theory sum rules on the light-cone*, Phys. Rev. D **101** (2020), no. 7 074035, [arXiv:1907.11092].
- [89] B.-Y. Cui, Y.-K. Huang, Y.-L. Shen, C. Wang, and Y.-M. Wang, *Precision calculations of $B_{d,s} \rightarrow \pi, K$ decay form factors in soft-collinear effective theory*, JHEP **03** (2023) 140, [arXiv:2212.11624].
- [90] J. Gao, C.-D. Lü, Y.-L. Shen, Y.-M. Wang, and Y.-B. Wei, *Precision calculations of $B \rightarrow V$ form factors from soft-collinear effective theory sum rules on the light-cone*, Phys. Rev. D **101** (2020), no. 7 074035, [arXiv:1907.11092].
- [91] B.-Y. Cui, Y.-K. Huang, Y.-M. Wang, and X.-C. Zhao, *Shedding new light on $R(D_{(s)}^{(*)})$ and*

- $|V_{cb}|$ from semileptonic $\bar{B}_{(s)} \rightarrow D_{(s)}^{(*)} \ell \bar{\nu}_\ell$ decays, Phys. Rev. D **108** (2023), no. 7 L071504, [arXiv:2301.12391].
- [92] **CLEO** Collaboration, J. P. Alexander et al., *First observation of $\bar{B} \rightarrow D^{(*)} \rho'^-$, $\rho'^- \rightarrow \omega \pi^-$* , Phys. Rev. D **64** (2001) 092001, [hep-ex/0103021].
- [93] D. Cabrera and R. Rapp, *The $\pi\rho$ Cloud Contribution to the ω Width in Nuclear Matter*, Phys. Lett. B **729** (2014) 67–71, [arXiv:1307.4001].
- [94] J. L. Lucio, M. Napsuciale, M. D. Scadron, and V. M. Villanueva, *The $\omega \rightarrow \rho\pi$ transition and $\omega \rightarrow 3\pi$ decay*, [hep-ph/9902349].
- [95] **Amsterdam-CERN-Nijmegen-Oxford** Collaboration, B. Jongejans et al., *Rare Decay Modes of $K^* (1420)$ and $K^* (892)$* , Nucl. Phys. B **139** (1978) 383.
- [96] R.-H. Li, C.-D. Lu, and H. Zou, *The $B(B_{(s)}) \rightarrow D_{(s)} P, D_{(s)} V, D_{(s)}^* P$ and $D_{(s)}^* V$ decays in the perturbative QCD approach*, Phys. Rev. D **78** (2008) 014018, [arXiv:0803.1073].